OPTIMIZATION OF SELECTING STRAIN MEASUREMENT LOCATIONS FOR DISTRIBUTED LOAD RECOVERY FROM STRAIN MEASUREMENTS

Hongna Dui[1] , Dongliang Liu[1], and Lixin Zhang[1]

[1] AVIC Chengdu Aircraft Design & Research Institute, Chengdu, China

Abstract: In order to solve the inverse problem of structural load distribution recovery from strain measurements, this paper focuses on how to optimize the number and locations of strain measurements, which is the key problem of influence coefficient method. An optimization procedure of selecting strain measurement locations centered on basis strains selection is proposed, which is matched with the Euclidean space method proposed in the previous study. Taking the load rams and fiber optic sensor data in a full-scale wing fatigue test as a case study, the feasibility of the optimization procedure is verified under the limited number of strain measurements. Furthermore, the load prediction accuracy under different numbers of strain measurements (unrestricted, 60 and 30) and different strain measurement errors (zero error, 2% random error, 5% random error, and actual error) are compared and analysed. It is verified that the optimization process proposed in this paper can provide quite high accuracy and robustness of load predictions and the load prediction accuracy is higher than traditional load calibration program based on strain bridges. It is recommended that the number of strain measurements be at least twice the number of basis load cases in practical applications.

Keywords: distributed load recovery; influence coefficient method; Euclidean space method; basis strains selection; basis cases selection

INTRODUCTION

For the inverse problem of structural load distribution recovery from strain measurements, the most widely used method is the influence coefficient method [1]-[3]. In the influence coefficient method, the accuracy of load distribution recovery depends on three main aspects, which are the selection of basis load cases, the selection of the number and location of strain measurements, and the reduction of ill-conditioning of the inverse matrix.

The authors have carried out an in-depth discussion and research on the selection of basis load cases and weakening of ill-conditioning of the inverse matrix in the previous study [4]-[5]. Distinguishing from the point loads method and load basis function method [1], the authors proposed a stepwise method based on Schmidt's orthogonalization of the maximum vertical distance to select the basis vectors from Euclidean space, which is called Euclidean space method[4]-[5] and used to select linearly independent basis cases from design load case database. Moreover, a set of engineering feasible distributed load recovery approach was established based on Euclidean space method. Taking

load rams and fiber optic sensor data of a aircraft wing fatigue test as a case study, it is verified that the load recovery approach has high prediction accuracy and robustness.

How to optimize the strain measurement locations with a limited number of strain measurements to maximize the accuracy and robustness of load distribution recovery is an engineering challenge and the focus of this paper. The literature [6] proposed the maximum determinant method (called D-optimal method), and the literature [7]-[8] suggested the use of sequential exchange algorithms to maximize the determinant by sequential augmentation and reduction of matrix. The literature [9] proposed the optimal condition number method (called C-optimal method) and verified that C-optimal method performs better than D-optimal method.

D-optimal method and C-optimal method are not suitable for direct application in distributed load recovery approach based on Euclidean space method [4], because the process needs to further select strain basis cases from the original strain space, and the criterion of selecting strain basis cases is not maximizing the determinant but can represent the strain space. Thus, even through the original strain space is conctructed with D-optimal method, the strain space is reconctructed with Euclidean space method, which does not guarantee that the determinant of the reconstructed matrix is the maximum. Therefore, an optimization method for selecting strain measurement locations that matches the distributed load recovery approach based on Euclidean space method is proposed in this paper.

INFLUENCE COEFFICIENT METHOD

Here, the influence coefficient method is briefly introduced. Based on linear elastic assumption, the influence coefficient method establishes mathematical relations between structural responses (such as displacement, stress, strain, etc.) and structural external loads, expressed as a linear matrix equation,

$$\{\boldsymbol{\varepsilon}_{g\times 1}\} = [\boldsymbol{A}_{g\times m}]\{\boldsymbol{\beta}_{m\times 1}\} \tag{1}$$

$$\{\boldsymbol{f}_{n\times 1}\} = [\boldsymbol{P}_{n\times m}]\{\boldsymbol{\beta}_{m\times 1}\} \tag{2}$$

where, $\{\cdot\}$ is a column vector, $[\cdot]$ is a matrix, $\{\boldsymbol{\varepsilon}\}$ and $\{\boldsymbol{f}\}$ is the strain vector and the load vector at an unknown load case, $[\boldsymbol{P}]$ is load distribution matrix at basis load cases, $[\boldsymbol{A}]$ is strain distribution matrix at basis load cases (referred to as the influence coefficient matrix), $\{\boldsymbol{\beta}\}$ is the linear coefficient, g is the number of strain measurements, m is the number of basis load cases, and n is the number of loading points.

According to the influence coefficient method, when $[\boldsymbol{P}]$ and $[\boldsymbol{A}]$ are determined and $\{\boldsymbol{\varepsilon}\}$ under any load condition is known, the load distribution $\{\boldsymbol{f}\}$ can be predicted by first calculating $\{\boldsymbol{\beta}\}$ by Equ. (1) and then substituting $\{\boldsymbol{\beta}\}$ into Equ. (2).

In practical application, $\{\boldsymbol{\varepsilon}\}$ obtained by physical test inevitably has measurement error. Assuming that strain measurement error obeys an independent normal distribution with a variance of σ^2, the variance-covariance matrix of $\{\boldsymbol{\beta}\}$ can be obtained by transforming Equ. (1),

$$\mathrm{var}(\{\boldsymbol{\beta}\}) = \sigma^2([\boldsymbol{A}]^T[\boldsymbol{A}])^{-1} \tag{3}$$

where, $([\boldsymbol{A}]^T[\boldsymbol{A}])^{-1}$ is referred to as the sensitivity of $[\boldsymbol{A}]$.

For a given strain measurement variance σ^2, the best combination of location, angle and number of strain measurements should be selected to minimize the sensitivity of $[\boldsymbol{A}]$ or maximize the determinant of $([\boldsymbol{A}]^T[\boldsymbol{A}])$ so as to improve the robustness of load recovery.

This paper focuses on how to optimize the strain measurement locations with a limited number of strain measurements based on the literature [4]. In practice, the number of strain measurements that a target structure can allow to be instrumented is usually limited, especially for the use of strain gauges. In addition, the optimal angle of strain measurements is not studied in this paper, and the direction of the maximum principal stress at load cases of interest is usually taken in engineering.

OPTIMIZATION OF SELECTING STRAIN MEASUREMENT LOCATIONS

An optimization procedure of selecting strain measurement locations centered on basis strains selection is proposed, shown as Figure 1, which is matched with the Euclidean space method proposed in the literature [4].

The optimization process is as follows:

Step 1): Construct load column space according to load distribution at design load cases, and stepwise select load basis cases based on Euclidean space method;

Step 2): Construct strain row space according to candidate strain set at design load cases, and stepwise select basis strains based on Euclidean space method;

Step 3): Construct strain column space according to basis strains set at design load cases, and stepwise select strain basis cases based on Euclidean space method, then influence coefficient matrix [$\boldsymbol{A}$] is determined;

Step 4): Calculate $det([\boldsymbol{A}]^T[\boldsymbol{A}])$, where *det* means determinant;

Step 5): Change the initial basis strain in step 2), and repeat step 2) ~ step 4), then select [$\boldsymbol{A}$] with the maximum $det([\boldsymbol{A}]^T[\boldsymbol{A}])$, and the final load distribution matrix [$\boldsymbol{P}$] is determined at the same time.

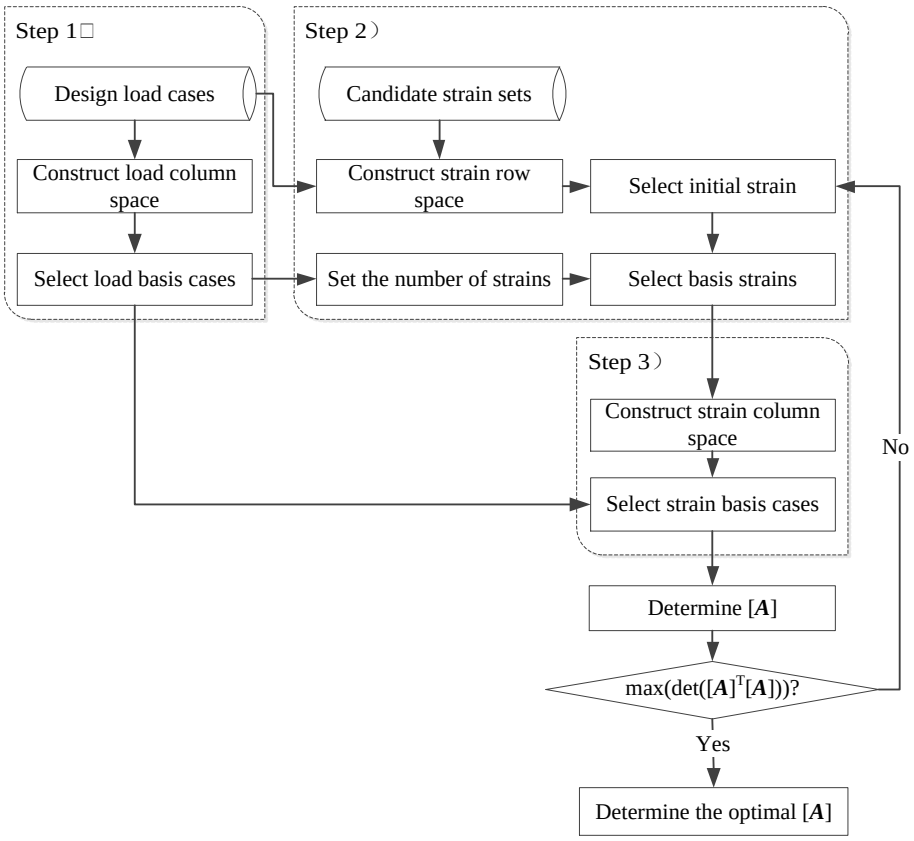

Figure 1: Flowchart of strain measurement locations optimization

Selection of load basis cases. The original load distribution matrix $[\boldsymbol{P}_{n,M}]=(\{\boldsymbol{f}_1\},\{\boldsymbol{f}_2\},...,\{\boldsymbol{f}_M\})$ is constructed according to load distribution at design load cases, where $\{\boldsymbol{f}_i\}$ is the column vector of load distribution at the *i*th load case, *M* is the number of design load cases, and *n* is the number of loading points.

Based on Euclidean space method [4]-[5], m_f load basis cases can be stepwise selected from the design load cases. Any load case can be linearly represented by this set of basis cases. The process is shown in Figure 2, and the general idea is to select the vector with the largest vertical distance from the current Euclidean space in turn to construct a new Euclidean space until all vectors are in that Euclidean space and the selected vectors are the basis cases.

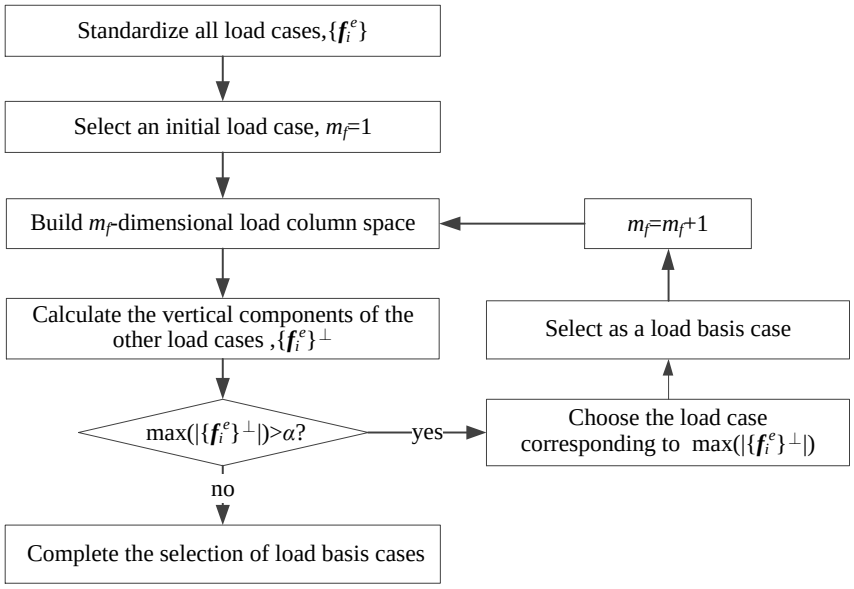

Figure 2: Flowchart of load basis cases selection

Selection of basis strains. The candidate strain set refers to the set of strain measurements that can be allowed to be arranged on the target structure, which in principle should be as dispersed as possible and have a large response to the loading region of interest.

The original strain distribution matrix $[\boldsymbol{A}_{G,M}]=(\{\boldsymbol{\alpha}_1\},\{\boldsymbol{\alpha}_2\},...,\{\boldsymbol{\alpha}_G\})^T$ is constructed based on the candidate strain set and the design load cases, where $\{\boldsymbol{\alpha}_j\}^T$ denotes strain row vector of the *j*th strain measurement at all design load cases, *M* is the number of design load cases, and *G* is the number of strain measurements in the candidate set.

With a strain selected as the initial basis strain, *g* basis strains can be stepwise selected from the candidate strain set to construct basis strain matrix $[\boldsymbol{A}_{g,M}]$ using Schmidt orthogonalization of the maximum vertical distance. The difference from selection of load basis cases is that the load column space is replaced with the strain row space, and the process is shown in Figure 3, where $\{\boldsymbol{\alpha}_j\}^T$ is represented by $<\boldsymbol{\alpha}_i>$ for ease of presentation.

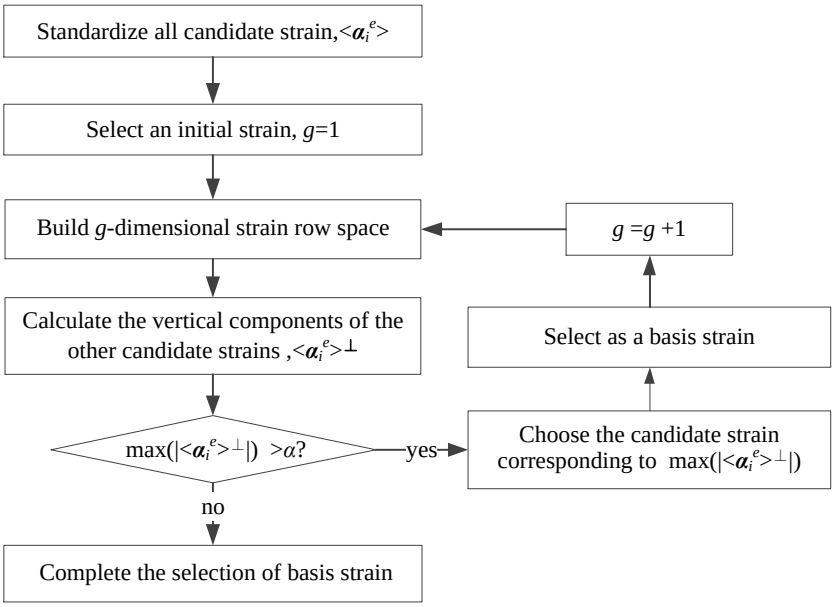

Figure 3: Flowchart of basis strains selection

Assuming that the number of strain measurements is limited to s in practical applications ($s \geq m_f$ should be satisfied), if $s \geq g$, the strain measurements can be directly taken as g basis strains; if $s \leq g$, the first s basis strains are selected according to the selecting order. For the convenience of presentation, g and s are no longer distinguished in the later section, and the basis strain matrix is denoted by $[A_{g,M}]$.

Selection of strain basis cases. According to the basis strain matrix $[\boldsymbol{A}_{g,M}]=(\{\boldsymbol{\varepsilon}_1\},\{\boldsymbol{\varepsilon}_2\},...,\{\boldsymbol{\varepsilon}_M\})$, where $\{\boldsymbol{\varepsilon}_i\}$ denotes the column vector of basis strain distribution at the ith load case, m_ε strain basis cases can be stepwise selected from the design load cases on the basis of the m_f load basis cases using Euclidean space method, and the influence coefficient matrix $[\boldsymbol{A}_{g,m_\varepsilon}]$ is constructed. The process is shown in Figure 4, and the key is that the strain basis cases need to include the load basis cases ($m_\varepsilon \geq m_f$). The detailed steps are described in the literature [4] and will not be repeated here.

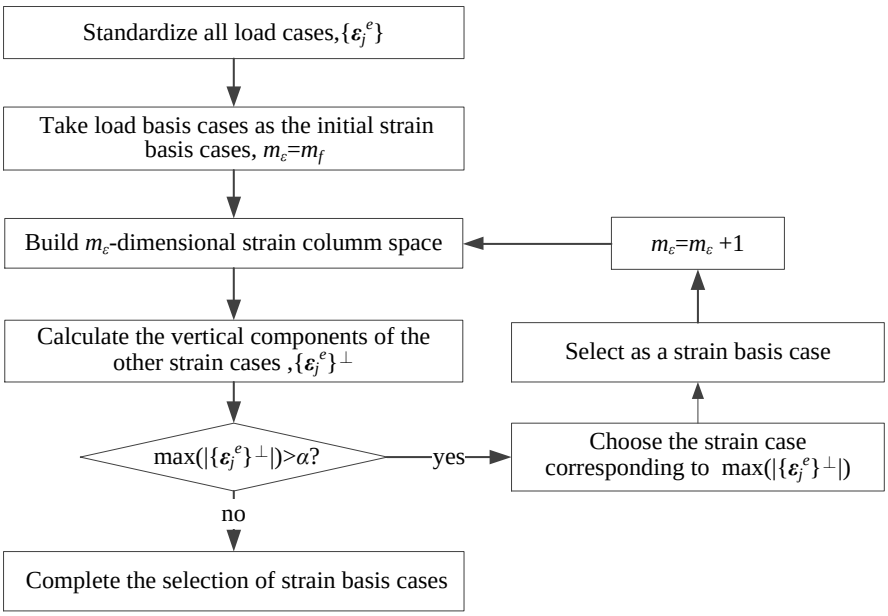

Figure 4: Flowchart of strain basis cases selection

CASE STUDY

Based on the load rams and fiber optic sensor data in a wing fatigue test in the literature [4], the feasibility of using the optimization procedure of selecting strain measurement locations with a limited number of strain measurements described as above is verified, and the load distribution under each test load condition is predicted with the measured strain distribution as input. Then, the predicted load distributions are compared with the actual values of load rams. The accuracy of load prediction is further compared and analyzed under different number limitations (unrestricted, 60 and 30) of strain measurements and different strain measurement error assumptions (zero error, 2% random error, 5% random error, and actual error).

In the fatigue test spectra, there are 749 independent load cases (i.e. M=749), 24 load rams that have applied loads through whiffletree to the lower wing surface (i.e. n=24), 4 main beams with fiber optic sensors along the span direction, and 116 effective strain measurements (excluding damaged/abnormal strains), which are used as the candidate strain set in this example (G=116). To eliminate the influence of strain measurement errors on the process of determining the influence coefficient matrix, the mean value of multiple measurements at the same load case is taken for each candidate strain measurement to obtain the original strain distribution matrix [$\boldsymbol{A}_{116,749}$].

Following the implementation steps described in Section 2, firstly, 23 load basis cases (m_f=23) are selected according to the distributed load matrix [$\boldsymbol{P}_{24,749}$], with the maximum wing bending moment case taken as the initial case and the error threshold taken as 1/10 of the minimum standard deviation after the standardization of all load vectors. Figure 5 illustrates the load distribution at the first two load basis cases with dimensionless axes, STA indicating the heading station and BL indicating the span station.

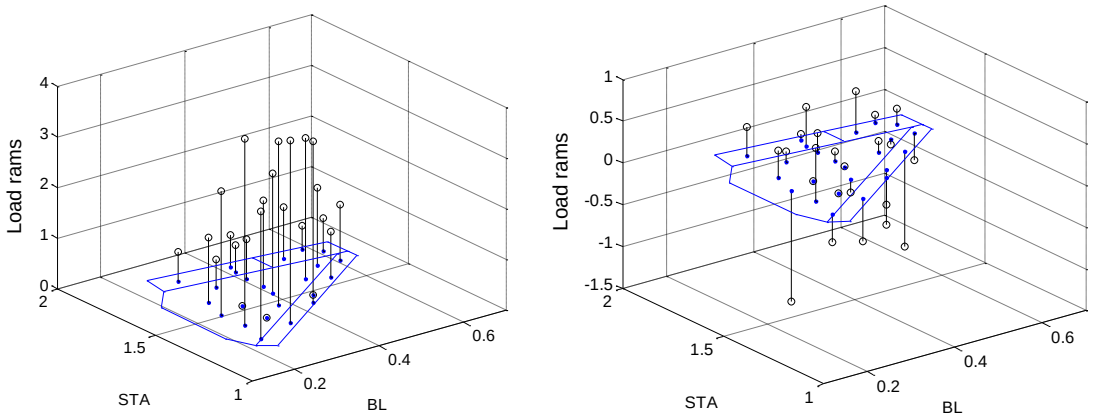

(a) Initial load basis case (b) The second load basis case

Figure 5: Illustration of load basis cases

Assuming that the number of strain measurements is limited to 60 (g=60), basis strains are stepwise selected according to the original strain distribution matrix [$\boldsymbol{A}_{116,749}$] with the strain measurement at the root of the lower stringer of a main beam as the initial strain and the error threshold taken as 1/10 of the minimum standard deviation after the standardization of all strain vectors, and the basis strain matrix [$\boldsymbol{A}_{60,749}$] is determined. The comparison of basis strains with the candidate strain set is shown in Figure 6, where the blue dots indicate strain measurements located at the upper stringer of the beam, and the red dots indicate strain measurements located at the lower stringer of the beam.

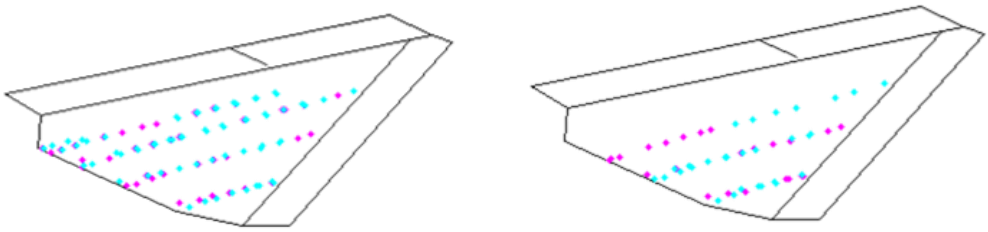

(a) 116 candidate strains (b) 60 basis strains

Figure 6: Comparisons of basis strains and candidate strain set

Then, 52 strain basis cases are stepwise selected according to the basis strain matrix $[\boldsymbol{A}_{60,749}]$, and a possible influence coefficient matrix $[\boldsymbol{A}_{60,52}]$ and basis load matrix $[\boldsymbol{P}_{24,52}]$ are determined. Next, $\det([\boldsymbol{A}]^{\mathrm{T}}[\boldsymbol{A}])$ is calculated, and the above process of basis strains selection (changing the selection of initial basis strain) and strain basis cases selection is repeated. Finally, the combination of basis strains and basis cases with the largest determinant is finally preferred, i.e., the optimal influence coefficient matrix and basis load matrix are determined.

Assuming that the load distribution $\{\boldsymbol{f}_i\}$ at test load cases is unknown and only the strain distribution $\{\boldsymbol{\varepsilon}_i\}$ at each case is known, the Tikhonov regularization method [10] is used to calculate $\{\boldsymbol{\beta}\}$ according to Eq. (1), and then $\{\boldsymbol{\beta}\}$ is substituted into Eq. (2) to predict the load rams at test load cases. Figure 7 illustrates the comparison between the predicted and actual values of load rams at two load cases (not the 52 strain basis cases), where the blue line indicates the actual value and the red line indicates the predicted value.

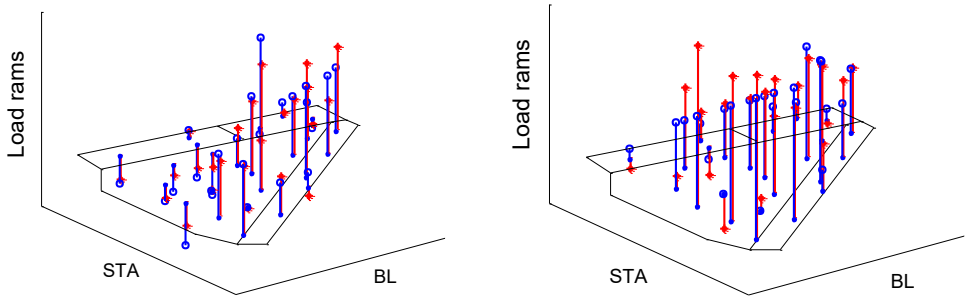

(a) Case 53# (b) Case 54#

Figure 7: Comparisons of predicted values and actualvalues of load rams

The overall component loads (including wing root shear/bending moment/torque, control surface shear/hinge moment) can be further calculated based on load predictions and positions of the actuatorload distribution recovery method.

The root mean square(RMS) error between the predicted and actual values of component loads is calculated to measure the accuracy of load distribution recovery method. The formula is as follows:

$$Error_{RMS} = \sqrt{\sum (f_{act} - f_{pred})^2} \Big/ \sqrt{\sum f_{act}^{\ 2}} \tag{4}$$

where, f_{act} is the actual load value and f_{pred} is the predicted load value.

Different numbers of strain measurements. In this section, the differences of load prediction accuracy for 749 load cases under different number limititations of strain measurements are compared, such as unrestricted, 60 and 30. In all instances, the strain distribution is assumed to be free of measurement error , i.e., the mean of multiple measurements at the same case is taken.

a) For the unrestricted number of strain measurements, the process is detailed in the literature [4], and the influence coefficient matrix $[\boldsymbol{A}_{116,82}]$ and the basis load matrix $[\boldsymbol{P}_{24,82}]$ are determined.

b) For the number of strain measurements limited to 60, the influence coefficient matrix [$\boldsymbol{A}_{60,52}$] and the basis load matrix [$\boldsymbol{P}_{24,52}$] are determined with the steps as described above.

c) For the number of strain measurements limited to 30, the influence coefficient matrix [$\boldsymbol{A}_{30,30}$]and the basis load matrix [$\boldsymbol{P}_{24,30}$] are determined with steps similar to b).

Figure 8 plots the predicted values versus actual values of component loads, with the actual values in the horizontal coordinates, the predicted values in the vertical coordinates. In the figure, each data point represents a load case and HM indicats hinge moment.

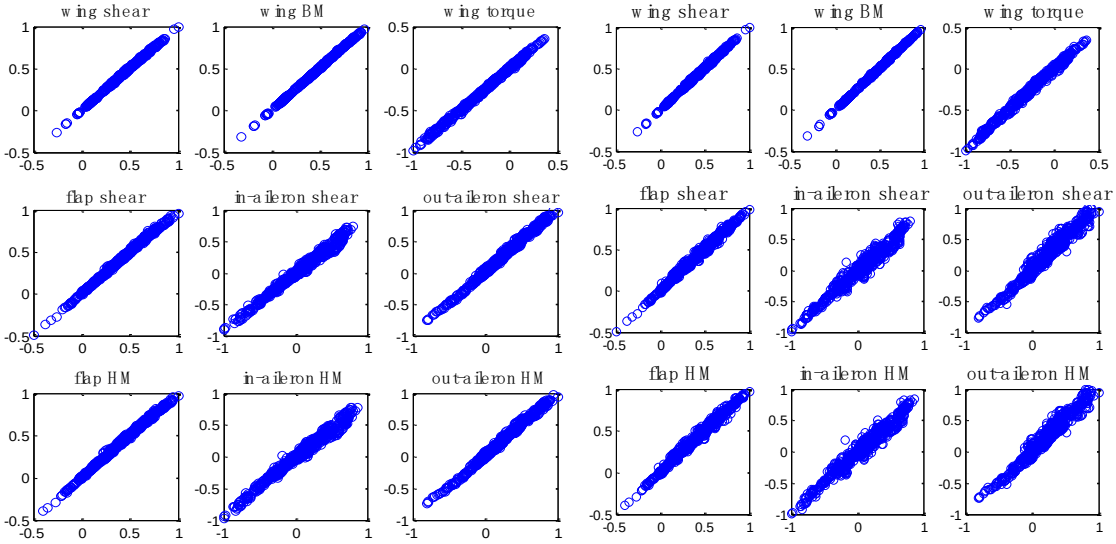

(a) 116 strain measurements (b) 60 strain measurements

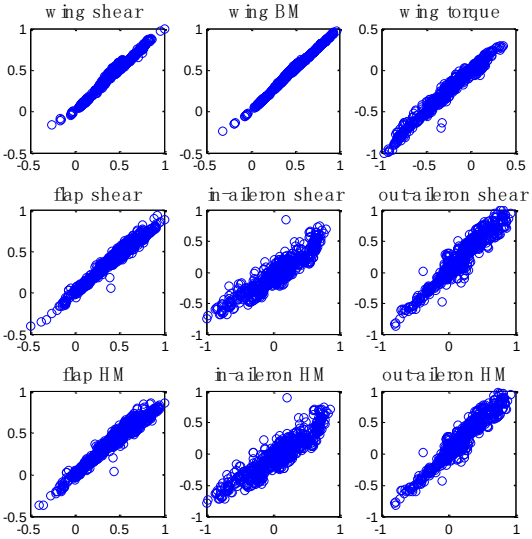

(c) 30 strain measurements

Figure 8: Comparisons of the predicted and actual values of component loads

The root-mean-square error between the predicted and actual values of component loads is calculated according to Equ. (4), and the results are compared in Figure 9.

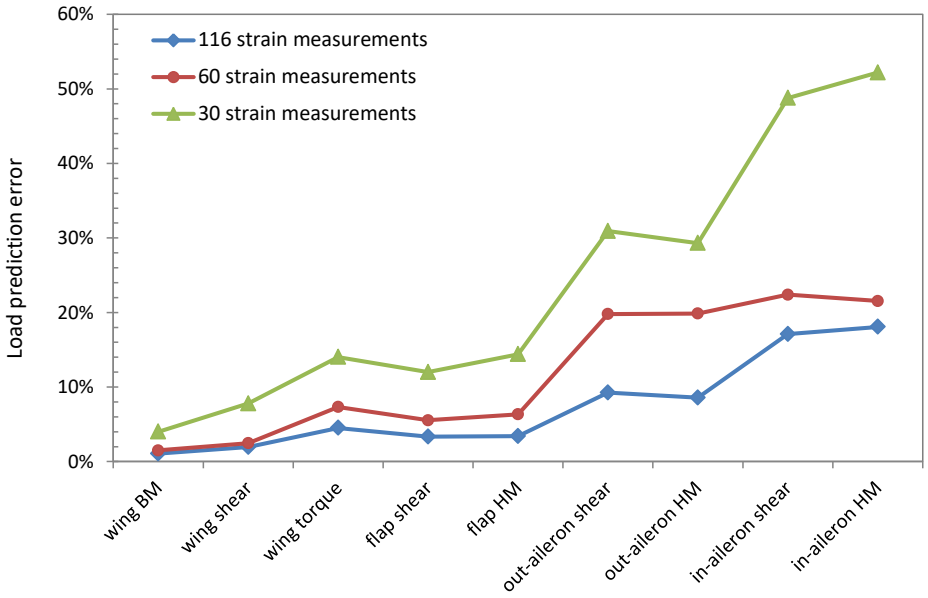

Figure 9: Comparisons of load prediction error under different numbers of strain measurements

Different strain measurement errors. In this section, the differences of load prediction accuracy for 749 load cases under different strain measurement errors are compared, such as zero error, 2% random error, 5% random error and actual measurement error. In all instances, the number of strain measurements is limited to 60.

a) zero measurement error, which means that strain distribution at each load case is taken as the mean value of multiple measurements at the same case;

b) 2% random error, which means that strain distribution at each load case introduces a 2% random error on the basis of the mean value;

c) 5% random error, which means that strain distribution at each load case introduces a 5% random error on the basis of the mean value;

d) Actual measurement error, which means that strain distribution at each load case is taken as the actual measured value (each case occurs multiple times in the load spectrum).

The root-mean-square error between the predicted and actual values of component loads is calculated according to Equ. (4), and the results are compared in Figure 10.

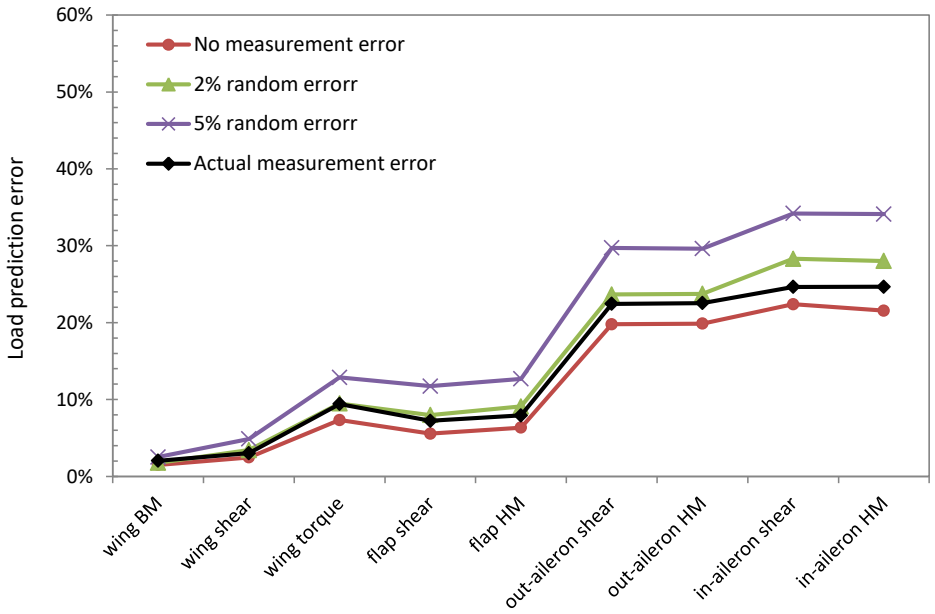

Figure 10: Comparisons of load prediction error under different strain measurement errors

Discussion. Through comparative analysis of the load recovery results in the case study, it can be seen that:

a) The component load prediction accuracy is ranked as: wing > flap > outer aileon > inner aileon. The poor accuracy of aileron load prediction is as expected, because the fiber optic sensors in this example are only arranged on the stringers of main beams, and the response of these strain measurements to the aileron load is small. If the aileron load is of interest, the strain measuremens in the aileron area should be increased, and then the accuracy of aileron load prediction will improve;

b) The accuracy of load recovery decreases as the number of strain measurements decreases, and it is recommended that the number of strain measurements be at least twice the number of basis load cases in practical applications.

c) The actual measurement error of strain is slightly less than 2% random error, so the accuracy of load recovery with actual measurement error is slightly better than 2% random error.

d) The load prediction accuracy based on strain distribution is higher than that of traditional component load calibration based on strain bridges. With the number of strain measurements limited to 60, the prediction error of component load with actual strain measurement error is <2% for wing root bending moment, <3% for wing root shear, and <10% for wing root torque; while for strain bridge-based component load calibration, the error of component load prediction is usually <5% for wing root bending moment, <10% for wing root shear, and >20% for wing root torque.

CONCLUSION

In this paper, an in-depth study on how to select strain measurement locations under the limited number of strain measurements is conducted, and an optimization procedure of of selecting strain measurement locations centered on basis strains selection is proposed, which is matched with the Euclidean space method proposed in the previous study. The optimization process is validated using the load rams and fiber optic sensor data in a wing fatigue test, and is summarized as follows:

a) The optimization process centered on basis strains selection and matched with Euclidean space method can provide highly accurate and robust load predictions, and the prediction accuracy is higher than that of the traditional strain bridge-based component load calibration method;

b) With the decrease of the number of strain measurements, the accuracy of load recovery is reduced. It is recommended that the number of strain measurements be at least twice the number of basis load cases in practical applications.

REFERENCES

[1] COATES C W, THAMBURAJ P. (2008). Inverse method using finite strain measurements to determine flight load distribution functions. *AIAA J. Aircraft*, 2008, 45(2): 366-370.
[2] ROMPPANEN, A. (2008). Inverse Load Sensing Method for Line Load Determination of Beam-Like Structures. *Tampere University of Technology*, Finland, 2008.
[3] NAKAMURA, T., IGAWA, H., and Kanda, A. (2012). Inverse identification of continuously distributed loads using strain data. *Aerospace Science and Technology*, 2012, 23: 75-84.
[4] DUI H N, LIU D L. (2021). An Inverse Approach Based on Euclidean Space for Determining Structural Load Distribution from Strain Measurements, *32nd Congress of the International Council of the Aeronautical Sciences*, September 2021.
[5] LIU D L, ZHANG L X. (2016). Fast simulation method for airframe analysis based on big data. *International Journal of Computational Materials Science & Engineering*, 2016, 05(04): 1650022.
[6] JOHN S T, DRAPER R C. (1975). D-optimality for regression designs: a review. *Technometrics*, 1975, 17: 15-24.
[7] GALIL Z, KIEFER J. (1980). Time- and Space- Saving Computer Methods, Related to Mitchell's DETMAX, for Finding D-Optimum Designs. *Technometrics*, 1980, 21: 301-313.
[8] JOHNSON M, NACHTSHEIM C J. (1983). Some Guidelines for Constructing Exact D-optimal Designs on Convex Design Spaces. *Technometrics*, 1983, 25 (3): 271-277.
[9] ZHANG M, QIU B B. (2019). Novel Computation Method of Reducing Ill-posedness for Structural Static Distributed Load Identification by Optimising Strain Gauge Locations. *Mechanical Systems and Signal Processing*, 2019, 124: 83-110.
[10] TIKHONOV A N, ARSENIN V Y. (1977). Solutions of ill-posed problems. New York: Wiley, 1977.